Supporting Information

Mechanism of Permanganate Promoted Dihydroxylation of Complex Diketopiperazines: Critical Roles of Counter-Cation and Ion-Pairing

Brandon E. Haines‡, Brandon M. Nelson†, Jessica M Grandner§, Justin Kim†, K. N. Houk§*, Mohammad Movassaghi†*, and Djamaladdin G. Musaev‡*

‡ Cherry L. Emerson Center for Scientific Computation and Department of Chemistry, Emory University, Atlanta, Georgia 30322, United States
†Department of Chemistry, Massachusetts Institute of Technology, Cambridge, Massachusetts 02139, United States
§Department of Chemistry and Biochemistry, University of California, Los Angeles, California 90095-1569, United States

Email: dmusaev@emory.edu, movassag@mit.edu, houk@ucla.edu

Table of Contents

1. **Supplementary data for the permanganate ion**

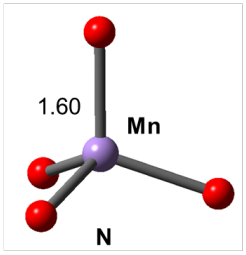

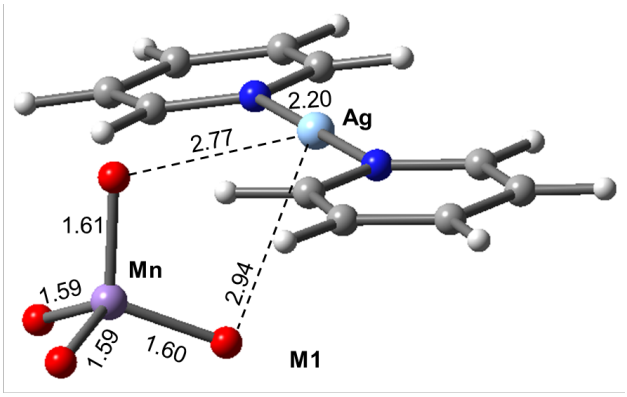

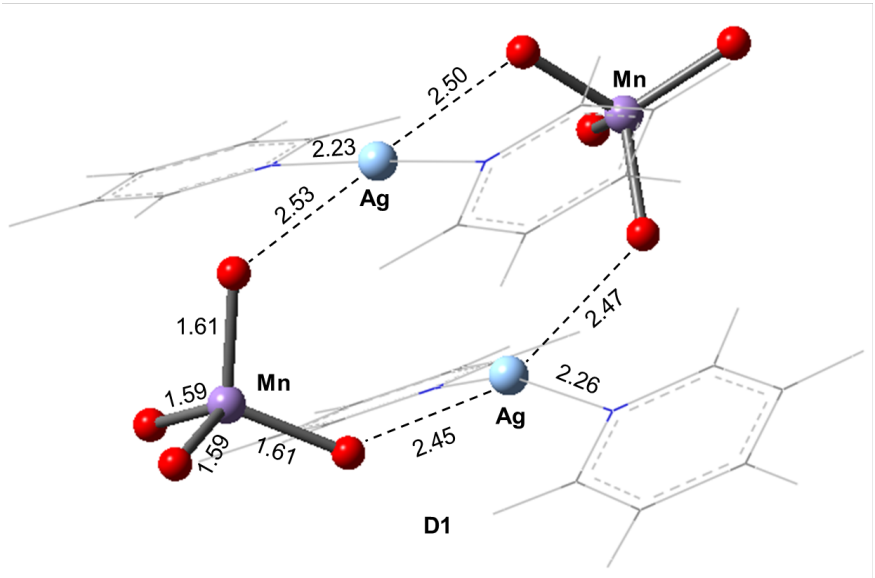

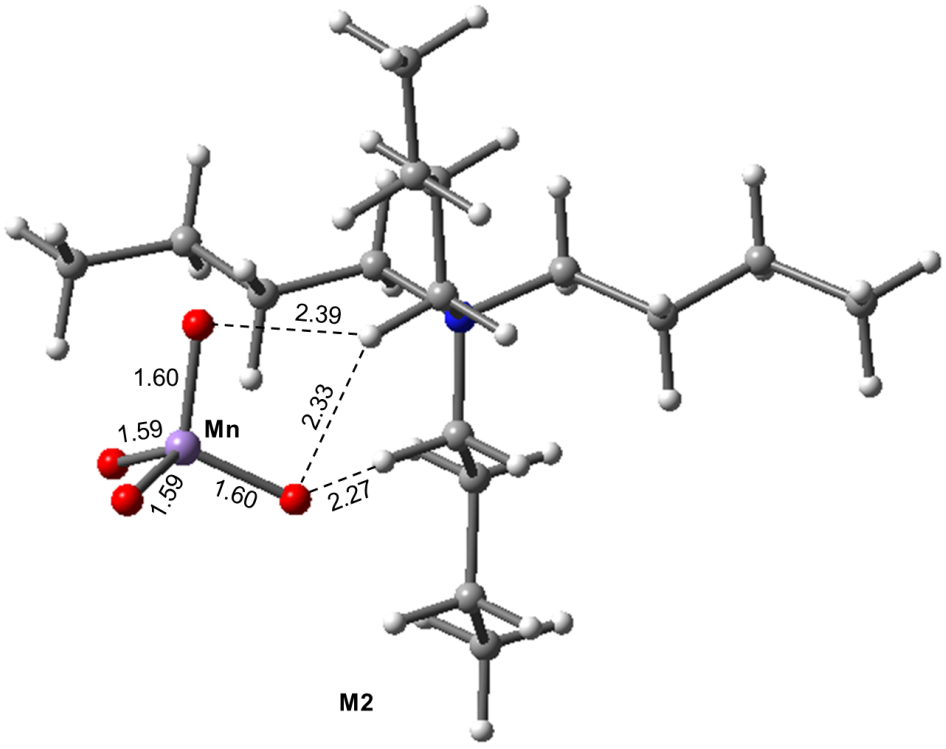

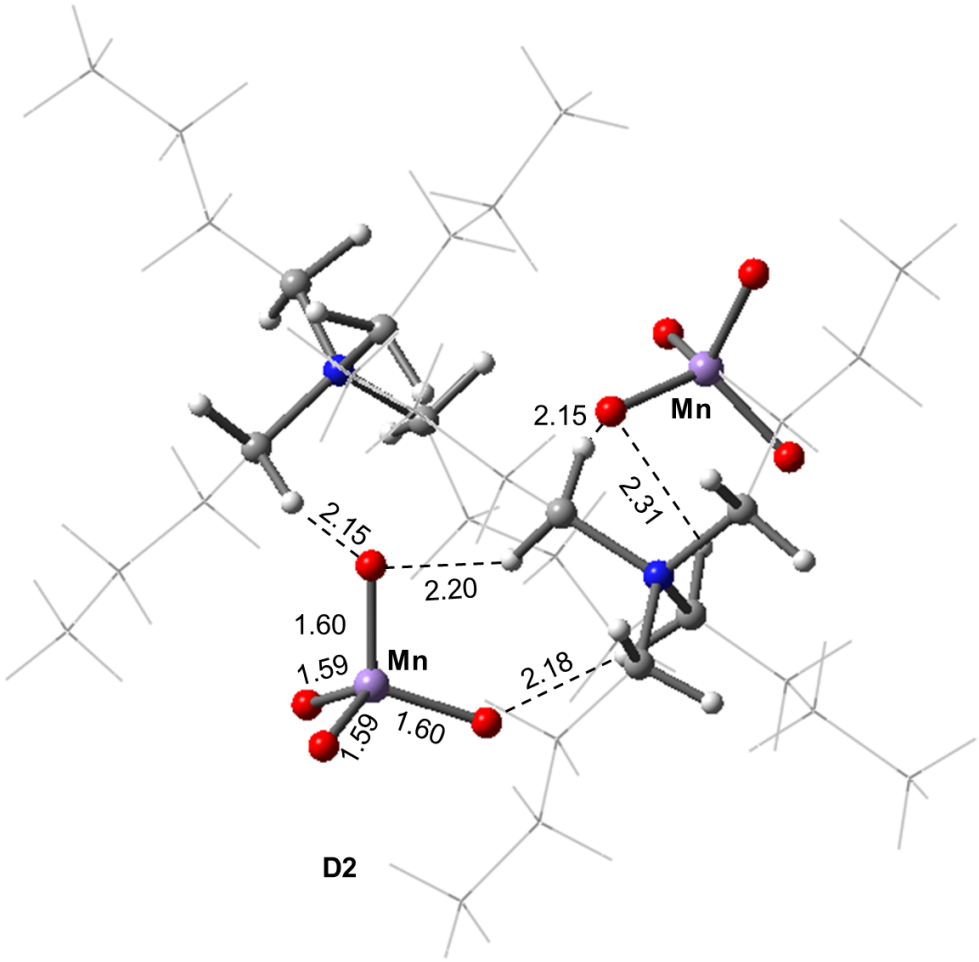

Figure S1. Optimized geometries for the model oxidants used in this study: **N**, **M1**, **D1**, **M2**, and **D2**. Bond distances are in Å.

In general, the ground electronic state of the permanganate ion (MnO_4^-) is well described as a closed shell singlet and the excited triplet states are very high in energy (~51 kcal/mol experimentally.[1] Popular DFT methods are known to underestimate the singlet-triplet energy splitting for first-row transition metal complexes [2-3] and more specifically the permanganate ion due to some multi-reference character in the ground state. We computed the singlet-triplet energy difference (from optimized structures at each level of theory) with hybrid (B3LYP, M06, wB97XD) and pure (BLYP, M06-L) density functionals with two basis sets, BS1 = LANL2DZ for Mn (with ECP) and 6-31g(d,p) for O and BS2 = 6-311+g(d,p) for Mn and O, to assess their performance in replicating the singlet-triplet energy splitting. (Table S1) We find that all of the methods examined here underestimate the singlet-triplet energy splitting and we find a wide range of values, ΔE = 17.6-35.2 kcal/mol. With the expectation that computed barriers involving the closed shell singlet and triplet states will be underestimated, we chose the B3LYP-D3BJ/BS1 level of theory with an empirical dispersion correction and implicit solvation model (PCM with dichloromethane as the solvent) and focus on relative trends in reactivity.

Table S1. The singlet-triplet energy difference the permanganate ion (MnO_4^-) with the B3LYP, M06, wB97XD, BLYP, and M06-L density functionals in conjunction with two basis sets (BSN), BS1 = LANL2DZ for Mn (with ECP) and 6-31g(d,p) for O and BS2 = 6-311+g(d,p) for Mn and O, to assess their performance in replicating the singlet-triplet energy splitting

DFT	BSN, where N = 1,2	E_{CSS} (hartree)	E_T (hartree)	ΔE (kcal/mol)
B3LYP	1	–404.808733	–404.777679	**19.5**
B3LYP	2	–1452.026918	–1451.993848	**20.8**
B3LYP-D3BJ	1	–404.810870	–404.779853	**19.5**
B3LYP-D3BJ, PCM = DCM	1	–404.889894	–404.858777	**19.5**
M06	1	–404.675444	–404.630697	**28.1**
M06	2	–1451.782316	–1451.741596	**25.6**
wB97XD	1	–404.652663	–404.624552	**17.6**
wB97XD	2	–1451.863337	–1451.835271	**17.6**
BLYP	1	–404.849881	–404.795620	**34.0**
BLYP	2	–1452.159189	–1452.103055	**35.2**
M06-L	1	–404.889796	–404.837247	**33.0**
M06-L	2	–1451.972304	–1451.920615	**32.4**

2. Supplementary data for oxidation of I

The structural features and BDEs of the full dimeric diketopiperazine substrate (+)-3 and model substrate **I** are generally consistent. (see Figure S2 and provided cartesian coordinates of these molecules)

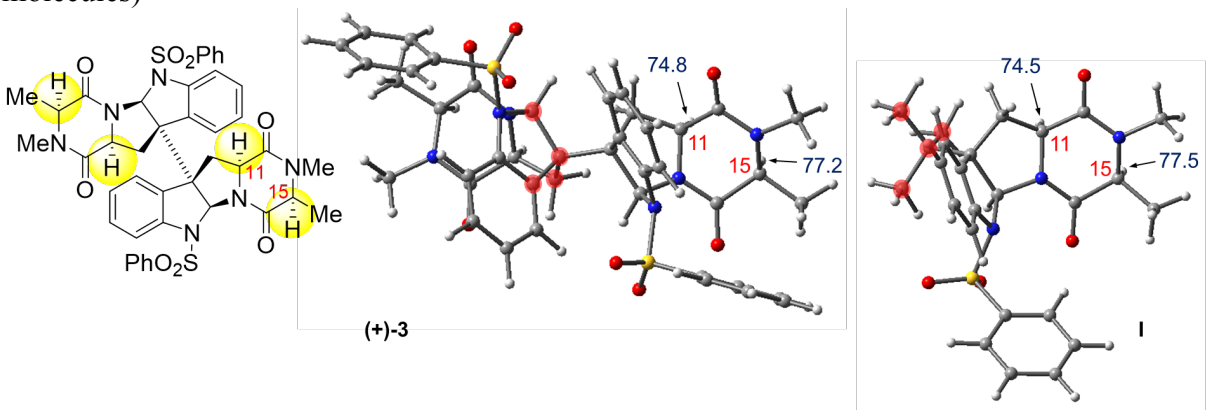

Figure S2. Comparison of the optimized structure of **(+)-3** and model substrate **I**. Computed bond dissociation energies (BDEs) are shown in blue and reported in kcal/mol.

The computed free barrier for interconversion of the permanganate ester (**I-3-N**) and alcohol (**I-3'N**) intermediates through transition state **I-3TS''-N** is 34.3 kcal/mol (Figure S3). This is high enough to suggest that this process is unlikely to occur to any significant degree.

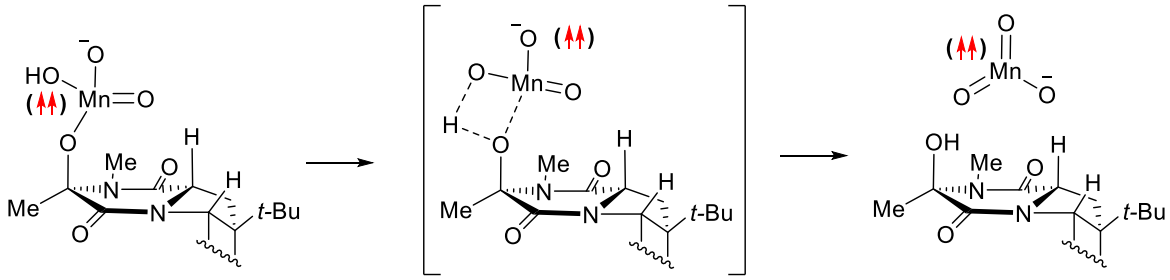

	I-3-N	**I-3TS''-N**	**I-3'-N**
ΔG/ΔH (kcal/mol)	0.0/0.0	34.3/33.4	21.6/20.6
	–42.7/–43.4	*–8.4/–9.9*	*–21.1/–22.8*

Figure S3. Computed energies for the interconversion of the permanganate ester (**I-3-N**) and alcohol (**I-3'N**) intermediates through transition state **I-3TS''-N**. Energies are calculated relative to **I-3-N** (and from **I-2-N** in italics) and are given as ΔG/ΔH in kcal/mol.

Presented in Figures S4-S7 are the computational data obtained for the reaction pathways following the first C–H abstraction of **I** by the permanganate ion starting at C^{11}. These data are consistent with the data for the pathways starting at C^{15} that are presented in the main text.

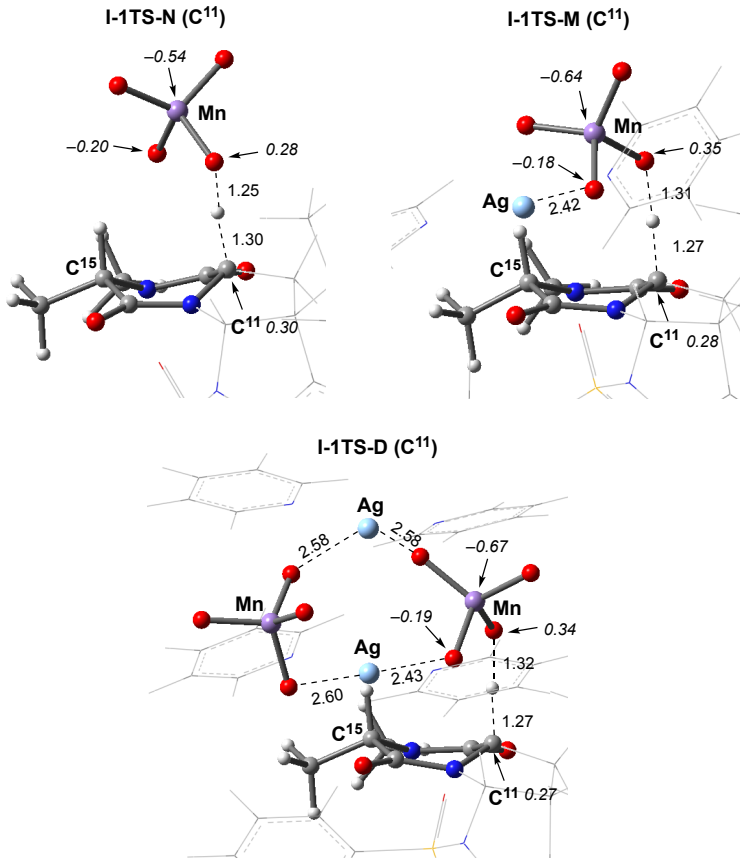

Figure S4. Optimized transition states for C–H abstraction at C11 (**I-1TS-X**) using the **N**, **M1**, and **D1** model oxidants. Bond distances are in Å and Mulliken spin density values in |e| are shown in italics.

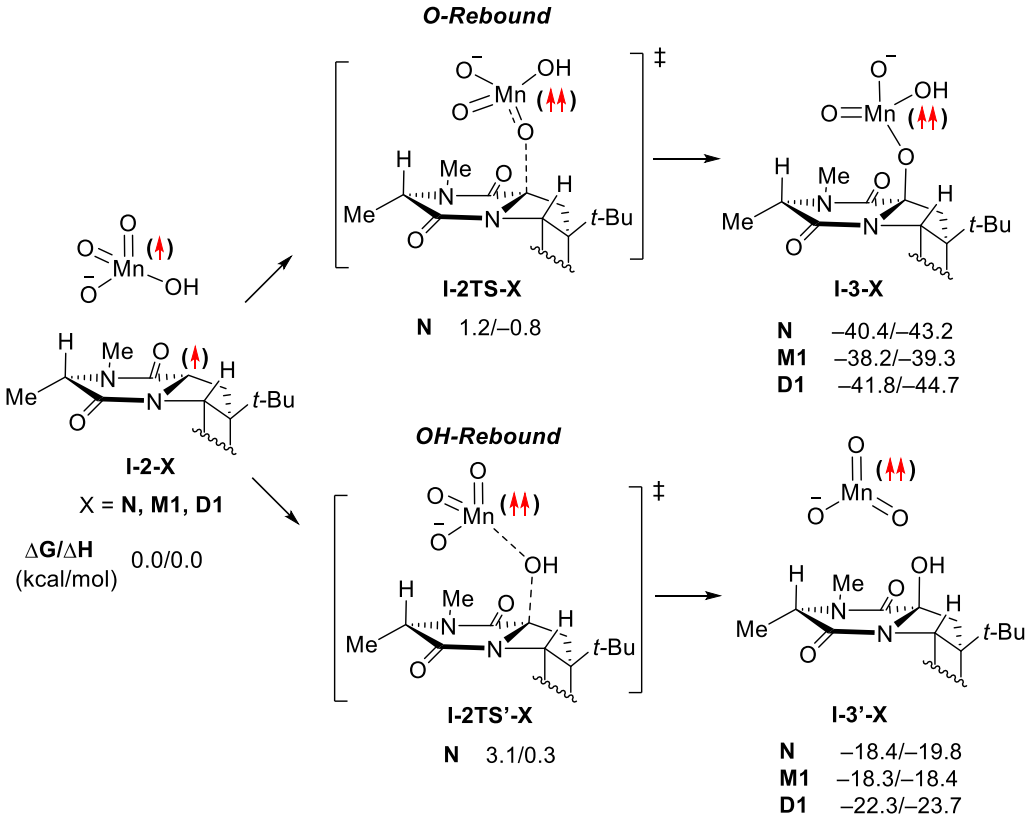

Figure S5. The examined O-rebound and OH-rebound pathways starting from oxidation at C^{11}. Energies are calculated relative to **I-2-X** and are given as ΔG/ΔH in kcal/mol. For sake of simplicity, here the schematic reaction pathway was shown only for model oxidant without counter-cation, i.e. for X = N.

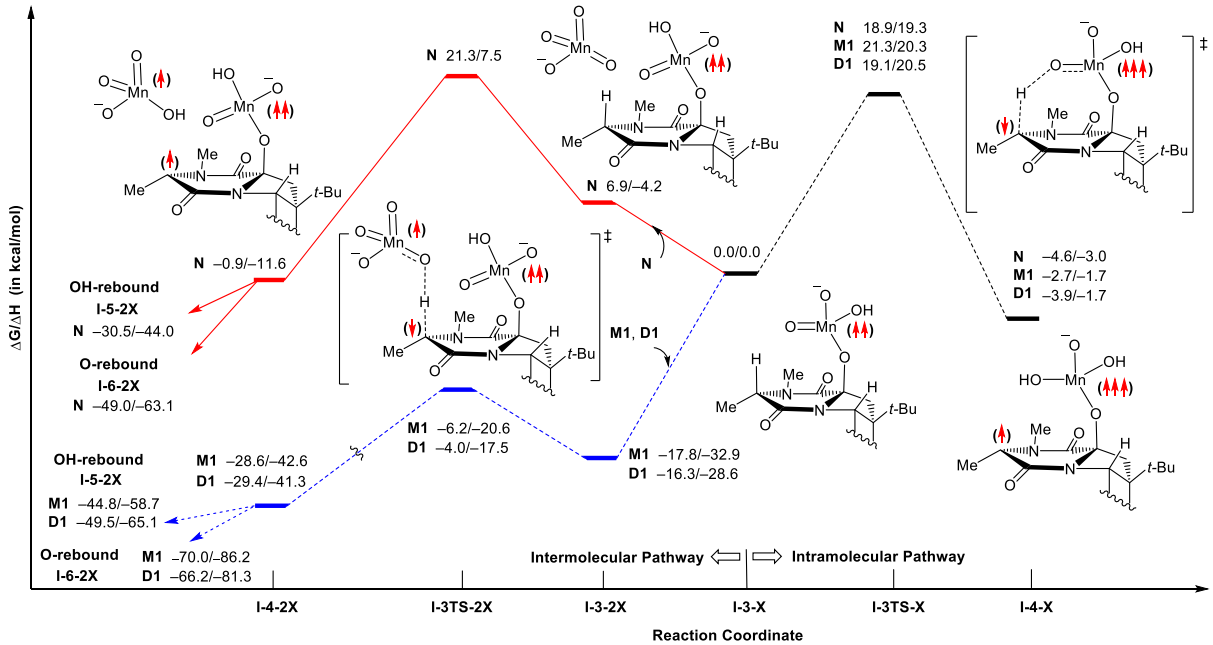

Figure S6. Schematic presentation intramolecular and intermolecular pathways of the C–H abstraction at the C^{15} position of the C^{11} permanganate intermediate **I-3-X** (i.e. the second C–H oxidation). All energies are calculated relative to the **I-3-X** + **X** dissociation limit. For simplicity, only the structures with **N** are depicted

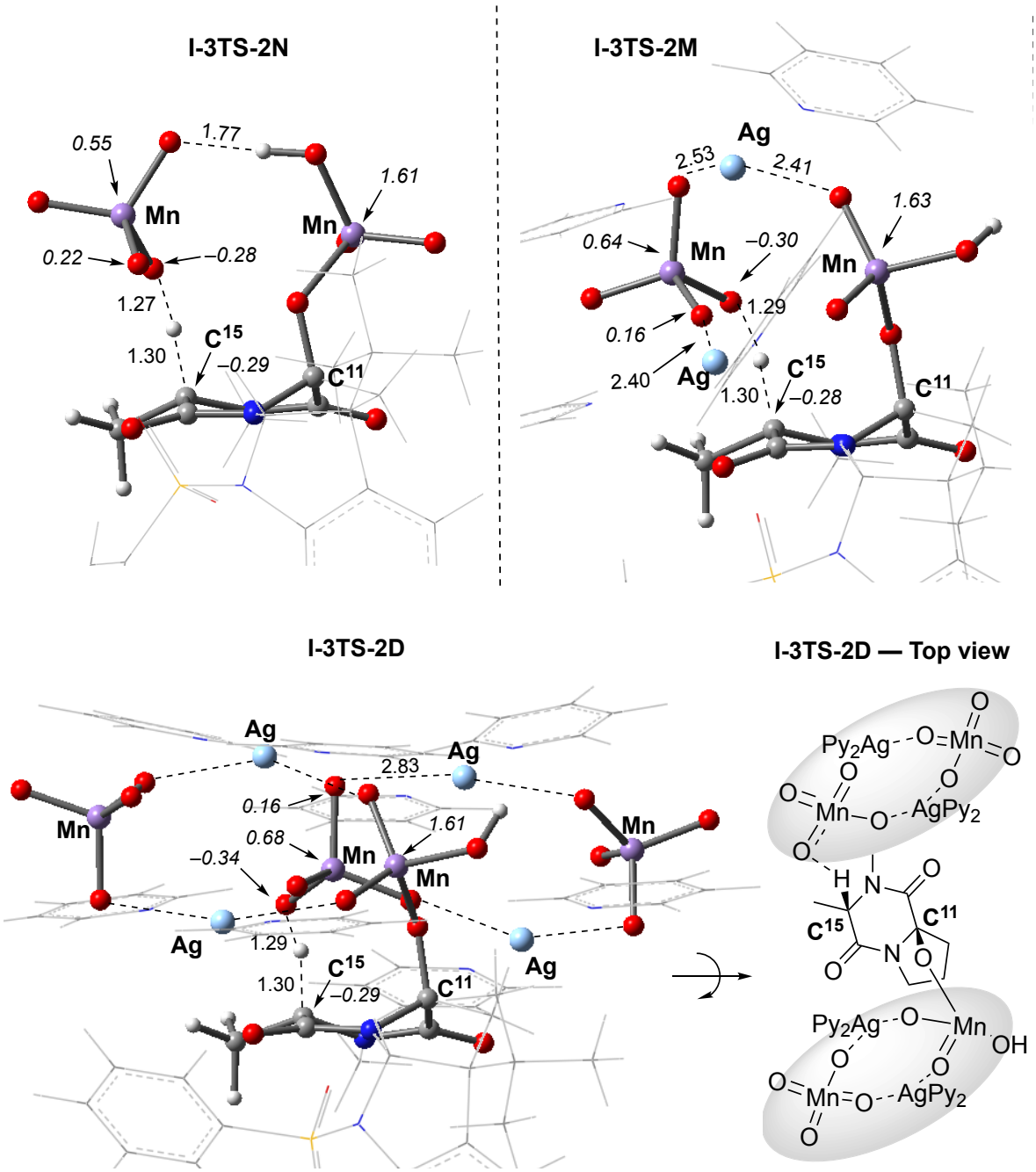

Figure S7. Optimized transition state structures for the second C–H abstraction through the intermolecular pathway (**I-3TS-2X**) starting from C^{11} for the model oxidants **N**, **M1**, and **D1**. Bond distances (in Å) and Mulliken spin density values (in |e|) are shown in italics. Some parts of the counter-cations have been removed from the visual representation for clarity.

3. **Supplementary data for oxidation of II**

Table S2. The calculated BDEs and energies for C–H abstraction at the C^{11} and C^{15} positions of **II** with model oxidants **N**, **M1**, and **D1**. For sake of simplicity, here the schematic reaction pathway is shown only for model oxidant **N** and for the C^{11}–H oxidation

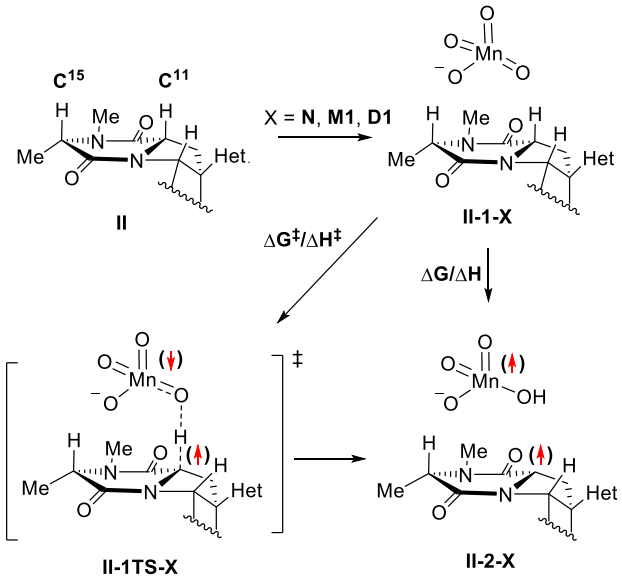

	C^{11}, BDE = 75.6 kcal/mol		**C^{15}**, BDE = 78.3 kcal/mol	
Ox.	ΔG‡/ΔH‡	ΔG/ΔH	ΔG‡/ΔH‡	ΔG/ΔH
N	12.3/12.6	–10.3/–9.0	11.6/11.4	–4.7/–2.5
M1	11.9/11.6	–11.7/–11.2	10.1/9.2	–8.8/–5.2
D1	10.9/10.1	–10.9/–10.4	11.3/9.7	–6.5/–4.8

4. Supplementary Data for Oxidation of III

III-1-N (C^{11}/C^{15})

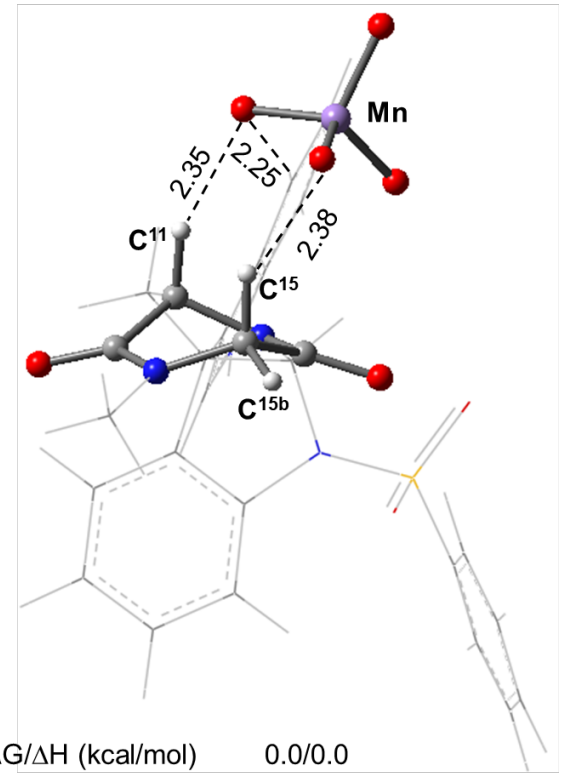

$\Delta G/\Delta H$ (kcal/mol) 0.0/0.0

III-1-N (C^{15b})

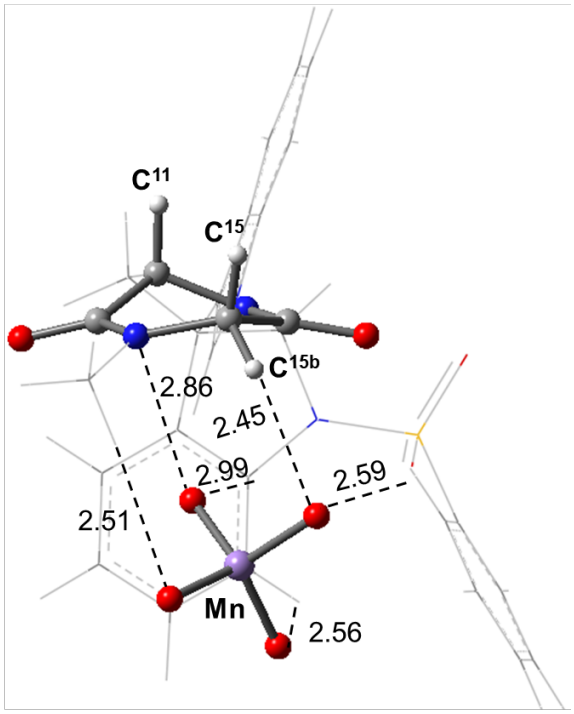

1.2/0.3

III-1-M1 (C^{11}/C^{15})

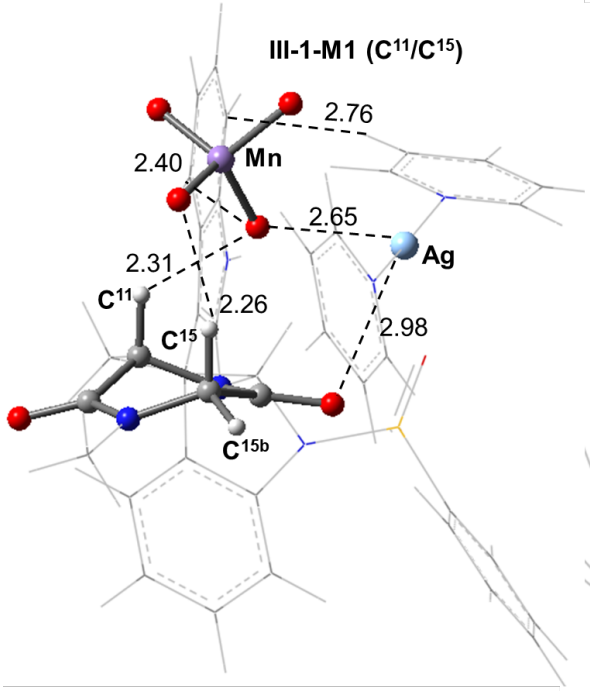

$\Delta G/\Delta H$ (kcal/mol) 0.0/0.0

III-1-M1 (C^{15b})

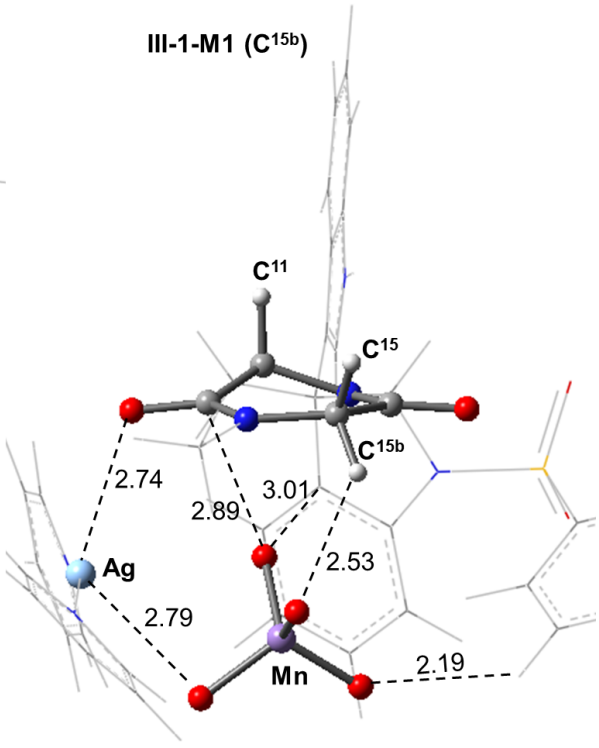

5.6/5.4

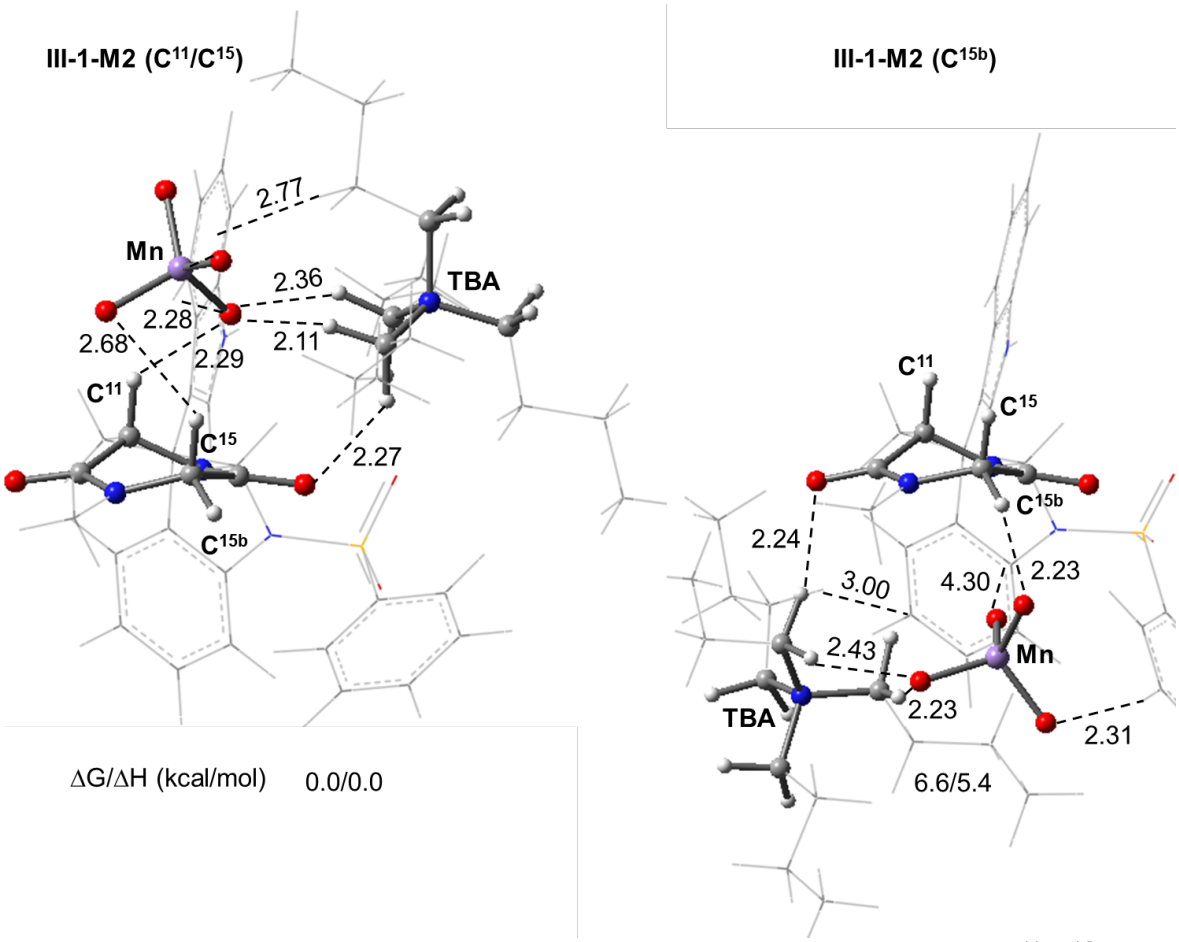

Figure S8. Optimized geometries for coordination of **N**, **M1** and **M2** to the C^{11}/C^{15} and C^{15b} faces of **III** (**III-1-X**). Bond distances are in Å and ΔG/ΔH are in kcal/mol.

5. Energies for Calculated Structures

Geometry optimizations and frequency calculations were performed with the Gaussian 09 suite of programs[4] at the B3LYP-D3/[6-31G(d,p) + Lanl2dz (Mn)] level of theory (called as B3LYP-D3/BS1) with the corresponding Hay-Wadt effective core potentials[5-7] for Mn and Grimme's empirical dispersion-correction for B3LYP (E_{BS1}).[8] Frequency analysis is used to characterize each minimum with zero imaginary frequencies and each transition state (TS) structures with only one imaginary frequency (ν_i in cm^{-1}). Bulk solvent effects are incorporated in all calculations (optimization of geometries, frequency and energy calculations) at the self-consistent reaction field polarizable continuum model (IEF-PCM) level of theory and with dichloromethane (DCM) as the solvent.[9-11] The final electronic energies (E_{BS2}) were re-computed at the B3LYP-D3/[6-311+G(d,p) + LANL2DZ (Mn)] level of theory (called as B3LYP-D3/BS2) by utilizing the geometries optimized at the B3LYP-D3/BS1 level. Thermal corrections for the free energy (G) and enthalpy (H) were calculated at the B3LYP-D3/BS1 level of theory and corrected to a solution standard state of 1M at 298.15 K.[12] These corrections were then applied to the energies calculated at the B3LYP-D3/BS2 level to afford the free energy and enthalpy values discussed in the text.

Table S3. Computed energies in hartree and vibrational frequency analysis for oxidant species and associated structures. (CSS = closed shell singlet, OSS = open shell singlet, D = doublet, T = triplet, Q = quintet)

Structure	E_{BS1}	E_{BS2}	H	G	$<S^2>$	ν_i (cm^{-1})
N-CSS	–404.889880	–404.989946	0.019081	–0.011688	-	-
N-T	–404.858935	–404.963259	0.017774	–0.015058	2.0311	-
Ag (Ag^+)	–642.286280	–642.405354	0.194639	0.140402	-	-
M1-CSS	–1047.217090	–1047.430098	0.215791	0.146083	-	-
M1-T	–1047.187842	–1047.403654	0.214582	0.144671	2.0332	-
M1H-D	–1047.857185	–1048.075910	0.226627	0.155720	0.7804	-
D1-CSS	–2094.499601	–2094.917137	0.433299	0.320252	-	-
D1H-D	–2095.140079	–2095.562499	0.443901	0.327212	0.7846	-
TBA$^+$	–686.104122	–686.239771	0.532527	0.457413	-	-
M2-CSS	–1091.014839	–1091.258111	0.553383	0.464190	-	-
M2-T	–1090.985597	–1091.231129	0.552037	0.459605	2.0316	-
M2H-D	–1091.652767	–1091.902392	0.564144	0.472564	0.7771	-
D2-CSS	–2182.084376	–2182.561973	1.109634	0.953739	-	-
D2H-D	–2182.722592	–2183.205931	1.120644	0.963700	0.7771	-
N'-CSS	–329.698012	–329.780559	0.014111	–0.015917	-	-
N'-OSS	–329.698055	–329.780917	0.013785	–0.016535	0.0828	-
N'-T	–329.692057	–329.779080	0.013272	–0.018876	2.0955	-
N'-Quintet	–329.653317	–329.745500	0.012440	–0.020968	6.0523	-
M1'-CSS	–972.025405	–972.218020	0.210732	0.141128	-	-
M1'-OSS	–972.025975	–972.218749	0.210482	0.140833	0.2906	-
M1'-T	–972.024993	–972.218914	0.210023	0.141198	2.1125	-
M1''-Q	–1944.173485	–1944.549793	0.423131	0.308763	6.0702	-
Toluene	–271.587685	–271.647864	0.135190	0.100430	-	-
Toluene-D	–270.934533	–270.995803	0.121442	0.088208	0.7832	-

Table S4. Computed energies in hartree and vibrational frequency analysis for the model substrates and associated structures. (CSS = closed shell singlet, OSS = open shell singlet, D = doublet, T = triplet, Q = quintet)

Structure	E_{BS1}	E_{BS2}	H	G	$<S^2>$	ν_i (cm^{-1})
I	–1833.575858	–1833.941943	0.542008	0.454653	-	-
I-C11-D	–1832.943375	–1833.310009	0.528847	0.440327	0.7552	-
I-C15-D	–1832.940258	–1833.305249	0.528884	0.441692	0.7556	-
I-C2-D	–1832.915593	–1833.280808	0.528513	0.441505	0.7557	-
I-C12-D	–1832.910448	–1833.277334	0.527420	0.439583	0.7542	-
I-C18-D	–1832.913735	–1833.281528	0.527735	0.440115	0.7563	-
I'-C11-OH	–1908.799078	–1909.192229	0.547051	0.457532	-	-
I'-C15-OH	–1908.766292	–1909.190991	0.547325	0.458732	-	-
I'' (diol)	–1983.996639	–1984.446307	0.552718	0.462804	-	-
(+)-3	–3351.393147	–3352.058351	0.827013	0.697466	-	-
(+)-3-C11-D	–3350.759721	–3351.425933	0.813736	0.681431	0.7552	-
(+)-3-C15-D	–3350.758044	–3351.422091	0.813854	0.683933	0.7572	-
II	–2038.949923	–2039.365714	0.540693	0.448376	-	-
II-C11-D	–2038.314852	–2038.731670	0.527194	0.432789	0.7553	-
II-C15-D	–2038.312579	–2038.727574	0.527396	0.434310	0.7564	-
III	–1999.628564	–2000.038117	0.510874	0.421880	-	-
III-C11-D	–1998.990936	–1999.400433	0.497448	0.405895	0.7549	-
III-C15-D	–1998.984922	–1999.394191	0.497699	0.407146	0.7568	-

Table S5. Computed energies in hartree and vibrational frequency analysis for the first C–H abstraction at C^{11} of **I** with **N**, **M1**, and **D1** and associated structures. (CSS = closed shell singlet, OSS = open shell singlet, D = doublet, T = triplet, Q = quintet)

Structure	E_{BS1}	E_{BS2}	H	G	$<S^2>$	ν_i (cm^{-1})
I-1-N-CSS	–2238.462427	–2238.954826	0.563757	0.462250	-	-
I-1TS-N-CSS	–2238.424754	–2238.919951	0.556612	0.456921	-	512.8i
I-3-N-CSS	–2238.522544	–2239.021962	0.563049	0.465821	-	-
I-1TS-N-OSS	–2238.434090	–2238.928213	0.556335	0.455980	0.6323	1797.2i
I-2-N-OSS	–2238.469796	–2238.967388	0.561063	0.457329	1.0262	-
I-2TS-N-OSS	–2238.465574	–2238.964322	0.560011	0.459922	0.7721	541.8i
I-3-N-OSS	–2238.526410	–2239.026980	0.562339	0.462944	0.6432	-
I-2TS'-N-OSS	–2238.451171	–2238.953972	0.558690	0.459350	1.0309	927.1i
I-3'-N-OSS	–2238.497867	–2238.998795	0.563075	0.460010	0.3650	-
I-1-N-T	–2238.431029	–2238.925970	0.562596	0.460891	2.032	-
I-1TS-N-T	–2238.423985	–2238.919449	0.558035	0.457584	2.0353	252.1i
I-2-N-T	–2238.469747	–2238.967290	0.561020	0.455693	2.0318	-
I-2TS-N-T	–2238.468419	–2238.967256	0.559673	0.457606	2.0781	357.8i
I-3-N-T	–2238.535541	–2239.037450	0.562300	0.461542	2.0302	-
I-2TS'-N-T	–2238.461808	–2238.964917	0.559071	0.458301	2.0564	528.6i
I-3'-N-T	–2238.498154	–2239.000371	0.562574	0.459465	2.084	-
I-1-M1-CSS	–2880.814320	–2881.415496	0.760238	0.624979	-	-
I-1TS-M1-OSS	–2880.788034	–2881.390773	0.753176	0.620484	0.6454	1480.1i
I-2-M1-T	–2880.825255	–2881.430179	0.757974	0.622403	2.0312	-
I-3-M1-T	–2880.887075	–2881.494301	0.759459	0.625677	2.0332	-
I-3'-M1-T	–2880.852196	–2881.461330	0.759871	0.624357	2.08	-
I-1-D1-CSS	–3928.100711	–3928.906835	0.978398	0.800831	-	-
I-1TS-D1-OSS	–3928.073579	–3928.881835	0.970948	0.792438	0.6445	1465.3i
I-2-D1-T	–3928.102686	–3928.915096	0.975492	0.793816	2.0379	-
I-3-D1-T	–3928.175859	–3928.988073	0.977223	0.800160	2.0322	-
I-3'-D1-T	–3928.140186	–3928.954734	0.977404	0.797902	2.1041	-

Table S6. Computed energies in hartree and vibrational frequency analysis for the first C–H abstraction at C^{15} of **I** with **N**, **M1**, and **D1** and associated structures. (CSS = closed shell singlet, OSS = open shell singlet, D = doublet, T = triplet, Q = quintet)

Structure	E_{BS1}	E_{BS2}	H	G	$<S^2>$	ν_i (cm^{-1})
I-1TS-N-OSS	–2238.436340	–2238.930916	0.556371	0.457453	0.5335	1735.5i
I-2-N-T	–2238.467166	–2238.964033	0.561375	0.457848	2.0316	-
I-2TS-N-T	–2238.467865	–2238.964990	0.560016	0.460181	2.0642	111.3i
I-3-N-T	–2238.532641	–2239.034023	0.562242	0.459867	2.0283	-
I-2TS'-N-T	–2238.451097	–2238.957426	0.559479	0.460962	2.048	182.9i
I-3'-N-T	–2238.501327	–2239.002008	0.562984	0.462251	2.0777	-
I-3TS''-N-T	–2238.477104	–2238.976129	0.557622	0.456586	2.0893	896.7i
I-1TS-M1-OSS	–2880.794192	–2881.395775	0.753312	0.621377	0.5249	1553.9i
I-2-M1-T	–2880.823478	–2881.426454	0.758148	0.621451	2.0319	-
I-3-M1-T	–2880.889285	–2881.497352	0.758823	0.625428	2.0309	-
I-3'-M1-T	–2880.852618	–2881.461362	0.759470	0.622482	2.0791	-
I-1TS-D1-OSS	–3928.073455	–3928.880188	0.970998	0.792250	0.5638	1447.5i
I-2-D1-T	–3928.097760	–3928.907556	0.975678	0.790854	2.0425	-
I-3-D1-T	–3928.169359	–3928.980536	0.976644	0.795455	2.0275	-
I-3'-D1-T	–3928.135084	–3928.948620	0.978022	0.798807	2.1022	-

Table S7. Computed energies in hartree and vibrational frequency analysis for the second C–H abstraction at C^{11} (after C–H abstraction and O-rebound at C^{15}) of **I** with **N**, **M1**, and **D1**. (CSS = closed shell singlet, OSS = open shell singlet, D = doublet, T = triplet, Q = quintet)

Structure	E_{BS1}	E_{BS2}	H	G	$<S^2>$	ν_i (cm^{-1})
I-3TS-N-T	–2238.493662	–2238.997660	0.554697	0.456301	2.7512	1371.2i
I-4-N-Q	–2238.529978	–2239.037854	0.559327	0.457327	6.0818	-
I-3-2N-T	–2643.437717	–2644.035305	0.584069	0.471640	2.0266	-
I-3TS-2N-T	–2643.408734	–2644.007021	0.576537	0.464319	2.5526	1856.8i
I-4-2N-Q	–2643.448271	–2644.048391	0.581344	0.465163	6.0553	-
I-5-2N-Q	–2643.483509	–2644.087231	0.582647	0.469723	6.0597	-
I-6-2N-Q	–2643.525081	–2644.125564	0.582382	0.471733	6.0591	-
I-3TS-M1-T	–2880.842883	–2881.455244	0.75155	0.619916	2.7778	959.8i
I-4-M1-Q	–2880.886605	–2881.500843	0.756451	0.622067	6.07	-
I-3-2M1-T	–3928.172454	–3928.978929	0.977572	0.800287	2.0319	-
I-3TS-2M1-T	–3928.146475	–3928.957375	0.969760	0.791322	2.6289	1582.2i
I-4-2M1-Q	–3928.184667	–3928.998959	0.974969	0.794385	6.0674	-
I-5-2M1-Q	–3928.204772	–3929.021862	0.975544	0.794489	6.151	-
I-6-2M1-Q	–3928.251490	–3929.066157	0.975944	0.798720	6.063	-
I-3TS-D1-T	–3928.134618	–3928.947759	0.969186	0.789293	2.7715	1015.1i
I-4-D1-Q	–3928.170177	–3928.986765	0.973858	0.789598	6.0847	-
I-3-2D1-T	–6022.739316	–6023.957779	1.413915	1.146519	2.0303	-
I-3TS-2D1-T	–6022.714449	–6023.934259	1.405887	1.136638	2.6236	1705.3i
I-4-2D1-Q	–6022.753172	–6023.975112	1.410699	1.137847	6.0647	-
I-5-2D1-Q	–6022.772700	–6023.997120	1.412321	1.143303	6.1195	-
I-6-2D1-Q	–6022.803384	–6024.029491	1.412153	1.142033	6.0621	-

Table S8. Computed energies in hartree and vibrational frequency analysis for the second C–H abstraction at C^{11} (after C–H abstraction and OH-rebound at C^{15}) of **I** with **N**, **M1**, and **D1**. (CSS = closed shell singlet, OSS = open shell singlet, D = doublet, T = triplet, Q = quintet).

Structure	E_{BS1}	E_{BS2}	H	G	$<S^2>$	ν_i (cm^{-1})
I-3TS'-N-T	–2238.480161	–2238.983552	0.555470	0.456418	2.6817	1237.1i
I-4'-N-Q	–2238.521255	–2239.026633	0.560497	0.456885	6.0817	-
I-5'-N-Q	–2238.572263	–2239.025723	0.560007	0.459035	6.0647	-
I-6'-N-Q	–2238.511371	–2239.088151	0.559907	0.460543	6.0971	-
I-3'-2N-T	–2643.437729	–2644.033291	0.584149	0.471724	2.0692	-
I-3TS'-2N-T	–2643.394612	–2643.992969	0.575101	0.462082	2.0566	712.2i
I-4'-2N-Q	–2643.462847	–2644.061261	0.582141	0.469919	6.0602	-
I-5'-2N-Q	–2643.522886	–2644.124855	0.583656	0.474133	6.0642	-
I-6'-2N-Q	–2643.519612	–2644.117991	0.583708	0.471247	6.0714	-
I-3TS'-M1-T	–2880.837476	–2881.446625	0.752474	0.620261	2.7054	1053.3i
I-4'-M1-Q	–2880.876214	–2881.488394	0.757136	0.620411	6.0851	-
I-5'-M1-Q	–2880.930426	–2881.548808	0.758454	0.623408	6.0712	-
I-6'-M1-Q	–2880.881292	–2881.497647	0.757731	0.623852	6.0836	-
I-3'-2M1-T	–3928.157353	–3928.969176	0.977904	0.797723	2.0617	-
I-3TS'-2M1-T	–3928.139033	–3928.950995	0.968841	0.789527	2.6365	1132.0i
I-4'-2M1-Q	–3928.181154	–3928.993899	0.974965	0.791857	6.0622	-
I-5'-2M1-Q	–3928.245040	–3929.061055	0.974776	0.797933	6.0817	-
I-6'-2M1-Q	–3928.240729	–3929.055314	0.977015	0.796788	6.0742	-

Table S9. Computed energies in hartree and vibrational frequency analysis for the second C–H abstraction at C^{15} (after C–H abstraction and O-rebound at C^{11}) of **I** with **N**, **M1**, and **D1**. (CSS = closed shell singlet, OSS = open shell singlet, D = doublet, T = triplet, Q = quintet)

Structure	E_{BS1}	E_{BS2}	H	G	$<S^2>$	ν_i (cm^{-1})
I-3TS-N-T	–2238.493510	–2238.998588	0.554160	0.452784	2.6148	1945.6i
I-4-N-Q	–2238.532573	–2239.039194	0.559324	0.455893	6.071	-
I-3-2N-T	–2643.441896	–2644.036397	0.583630	0.469882	2.0264	-
I-3TS-2N-T	–2643.415955	–2644.011128	0.577037	0.467607	2.5775	1758.2i
I-4-2N-Q	–2643.448895	–2644.046445	0.581984	0.467502	6.0585	-
I-5-2N-Q	–2643.496854	–2644.098714	0.582525	0.472602	6.0581	-
I-3TS-M1-T	–2880.844635	–2881.453964	0.751441	0.619287	2.5437	2328.8i
I-4-M1-Q	–2880.881435	–2881.494039	0.756542	0.621181	6.0811	-
I-3-2M1-T	–3928.167796	–3928.978005	0.976459	0.797014	2.0332	-
I-3TS-2M1-T	–3928.139670	–3928.950896	0.968863	0.788436	2.6093	1696.0i
I-4-2M1-Q	–3928.177778	–3928.991427	0.974360	0.793280	6.0693	-
I-5-2M1-Q	–3928.213402	–3929.028665	0.975770	0.797168	6.1253	-
I-3TS-D1-T	–3928.133270	–3928.947291	0.969150	0.789813	2.8125	986.2i
I-4-D1-Q	–3928.170031	–3928.987692	0.974127	0.793488	6.0778	-
I-3-2D1-T	–6022.734627	–6023.954253	1.414043	1.143405	2.0313	-
I-3TS-2D1-T	–6022.708425	–6023.928725	1.406196	1.137562	2.7299	1630.2i
I-4-2D1-Q	–6022.749507	–6023.972188	1.411627	1.140591	6.0671	-
I-5-2D1-Q	–6022.765286	–6023.990600	1.412566	1.142528	6.122	-

Table S10. Computed energies in hartree and vibrational frequency analysis for the first C–H abstraction at C^{11} and C^{15} of **II** with **N**, **M1**, and **D1** and associated structures. (CSS = closed shell singlet, OSS = open shell singlet, D = doublet, T = triplet, Q = quintet)

Structure	E_{BS1}	E_{BS2}	H	G	$<S^2>$	ν_i (cm^{-1})
C^{11}–H						
II-1-N-CSS	–2443.831462	–2444.378921	0.562319	0.456783	-	-
II-1TS-N-OSS	–2443.802317	–2444.351250	0.554681	0.448666	0.6259	1771.1i
II-2-N-T	–2443.840488	–2444.391031	0.560025	0.452537	2.0288	-
II-1-M1-CSS	–3086.185765	–3086.840675	0.759120	0.621095	-	-
II-1TS-M1-OSS	–3086.159082	–3086.814996	0.751864	0.614398	0.6532	1435.5i
II-2-M1-T	–3086.198996	–3086.856123	0.756666	0.617836	2.0322	-
II-1-D1-CSS	–4133.474370	–4134.332741	0.976760	0.794836	-	-
II-1TS-D1-OSS	–4133.449194	–4134.309653	0.969698	0.789096	0.6496	1393.6i
II-2-D1-T	–4133.485440	–4134.347125	0.974606	0.791859	2.043	-
C^{15}–H						
II-1TS-N-OSS	–2443.804028	–2444.353158	0.554801	0.449466	0.5202	1735.6i
II-2-N-T	–2443.827232	–2444.380267	0.559748	0.450583	2.0329	-
II-1TS-M1-OSS	–3086.162246	–3086.818676	0.751783	0.615123	0.5574	1508.1i
II-2-M1-T	–3086.187515	–3086.846426	0.756526	0.612892	2.0352	-
II-1TS-D1-OSS	–4133.450477	–4134.310189	0.969731	0.790319	0.5876	1435.7i
II-2-D1-T	–4133.475146	–4134.337880	0.974253	0.789580	2.0378	-

Table S11. Computed energies in hartree and vibrational frequency analysis for the first C–H abstraction at C^{11}, C^{15}–H^a and C^{15}–H^b of **III** with **N**, **M1**, and **M2** and associated structures. (CSS = closed shell singlet, OSS = open shell singlet, D = doublet, T = triplet, Q = quintet)

Structure	E_{BS1}	E_{BS2}	H	G	$<S^2>$	ν_i (cm^{-1})
C^{11}–H						
III-1-N-CSS	–2404.510513	–2405.050746	0.532441	0.429035	-	-
III-1TS-N-OSS	–2404.481898	–2405.023461	0.525047	0.421651	0.6289	1784.6i
III-2-N-T	–2404.517292	–2405.061484	0.530105	0.425980	2.0313	-
III-1-M1-CSS	–3046.863118	–3047.510444	0.729269	0.592449	-	-
III-1TS-M1-OSS	–3046.837587	–3047.486037	0.722022	0.588167	0.6571	1487.6i
III-2-M1-T	–3046.873583	–3047.522868	0.727030	0.590343	2.0318	-
III-1-M2-CSS	–3090.662243	–3091.339963	1.067542	0.911615	-	-
III-1TS-M2-OSS	–3090.636535	–3091.315096	1.059896	0.906350	0.6196	1600.7i
III-2-M2-T	–3090.673165	–3091.352474	1.065631	0.911326	2.0313	-
C^{15}–H^a						
III-1TS-N-OSS	–2404.480391	–2405.022234	0.525168	0.423786	0.5212	1864.6i
III-2-N-T	–2404.502364	–2405.048250	0.530037	0.423900	2.0345	-
III-1TS-M1-OSS	–3046.838201	–3047.486475	0.722115	0.587561	0.5533	1714.9i
III-2-M1-T	–3046.860007	–3047.511640	0.726669	0.584866	2.0348	-
III-1TS-M2-OSS	–3090.638069	–3091.316577	1.060472	0.907227	0.5151	1759.6i
III-2-M2-T	–3090.656717	–3091.339014	1.065671	0.907402	2.0354	-
C^{15}–H^b						
III-1-N-CSS	–2404.511246	–2405.050207	0.532337	0.430406	-	-
III-1TS-N-OSS	–2404.478769	–2405.020039	0.524959	0.424656	0.5313	1951.7i
III-2-N-T	–2404.511643	–2405.054074	0.530676	0.425588	2.0329	-
III-1-M1-CSS	–3046.853665	–3047.501616	0.729061	0.592489	-	-
III-1TS-M1-OSS	–3046.818896	–3047.469189	0.721862	0.586588	0.6334	1786.7i
III-2-M1-T	–3046.847206	–3047.500442	0.726705	0.586694	2.0345	-
III-1-M2-CSS	–3090.655036	–3091.331627	1.067779	0.913744	-	-
III-1TS-M2-OSS	–3090.621822	–3091.299705	1.060288	0.908186	0.4966	1920.6i
III-2-M2-T	–3090.653258	–3091.333391	1.065820	0.909332	2.0337	-

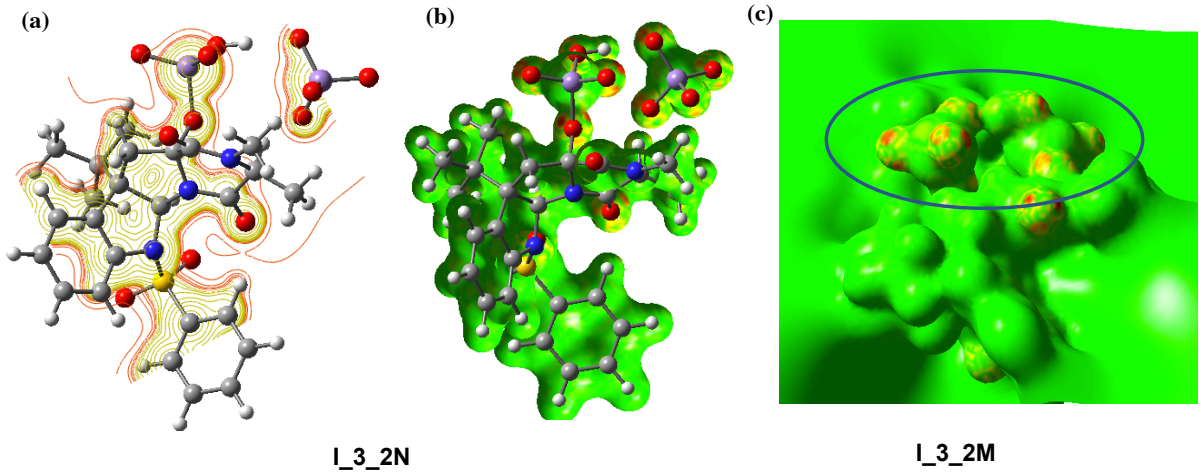

Figure S9. (a) Contour plot and (b) electrostatic potential map of the **I_3_2N** intermediate, showing no positive interaction between the MnO_4-units, and (c) electrostatic potential map of the **I_3_2M** intermediate, showing attractive interaction between the MnO_4-units.

7. References

1. Gardner, K. A.; Kuehnert, L. L.; Mayer, J. M. Hydrogen Atom Abstraction by Permanganate: Oxidations of Arylalkanes in Organic Solvents. *Inorg. Chem.* **1997**, *36*, 2069-2078.
2. Ghosh, A.; Taylor, P. R. High-Level Ab Initio Calculations on the Energetics of Low-Lying Spin States of Biologically Relevant Transition Metal Complexes: First Progress Report. *Curr. Opin. Chem. Biol.* **2003**, *7*, 113-124.
3. Yang, T. H.; Quesne, M. G.; Neu, H. M.; Reinhard, F. G. C.; Goldberg, D. P.; de Visser, S. P. Singlet Versus Triplet Reactivity in an Mn(V)-Oxo Species: Testing Theoretical Predictions against Experimental Evidence. *J. Am. Chem. Soc.* **2016**, *138*, 12375-12386.
4. Creary, X.; Butchko, M. A. Beta-Trimethylsilyl Cyclopropylcarbenes. *J. Org. Chem.* **2001**, *66*, 1115-1121.
5. Hay, P. J.; Wadt, W. R. Abinitio Effective Core Potentials for Molecular Calculations - Potentials for the Transition-Metal Atoms Sc to Hg. *J. Chem. Phys.* **1985**, *82*, 270-283.
6. Hay, P. J.; Wadt, W. R. Abinitio Effective Core Potentials for Molecular Calculations - Potentials for K to Au Including the Outermost Core Orbitals. *J. Chem. Phys.* **1985**, *82*, 299-310.
7. Wadt, W. R.; Hay, P. J. Abinitio Effective Core Potentials for Molecular Calculations - Potentials for Main Group Elements Na to Bi. *J. Chem. Phys.* **1985**, *82*, 284-298.
8. Grimme, S.; Antony, J.; Ehrlich, S.; Krieg, H. A Consistent and Accurate Ab Initio Parametrization of Density Functional Dispersion Correction (DFT-D) for the 94 Elements H-Pu. *J. Chem. Phys.* **2010**, *132*, 154104.
9. Cances, E.; Mennucci, B.; Tomasi, J. A New Integral Equation Formalism for the Polarizable Continuum Model: Theoretical Background and Applications to Isotropic and Anisotropic Dielectrics. *J. Chem. Phys.* **1997**, *107*, 3032-3041.
10. Mennucci, B.; Tomasi, J. Continuum Solvation Models: A New Approach to the Problem of Solute's Charge Distribution and Cavity Boundaries. *J. Chem. Phys.* **1997**, *106*, 5151-5158.

11. Scalmani, G.; Frisch, M. J. Continuous Surface Charge Polarizable Continuum Models of Solvation. I. General Formalism. *J. Chem. Phys.* **2010**, *132*, 114110-114124.
12. Essafi, S.; Tomasi, S.; Aggarwal, V. K.; Harvey, J. N. Homologation of Boronic Esters with Organolithium Compounds: A Computational Assessment of Mechanism. *J. Org. Chem.* **2014**, *79*, 12148-12158.